Abstract. The well-observed spiral galaxy M101 was considered. The radial distributions of oxygen abundances determined in three different ways (with the classic T_e – method, with the R_{23} – method, and with the P – method) were compared. It was found that the parameters (the central oxygen abundance and the gradient) of the radial $(O/H)_P$ abundance distribution are close to those of the $(O/H)_{T_e}$ abundance distribution. The parameters of the $(O/H)_{R_{23}}$ abundance distribution differ significantly from those of the $(O/H)_{T_e}$ abundance distribution: the central $(O/H)_{R_{23}}$ oxygen abundance is higher by around 0.4dex and the gradient is steeper by a factor of around 1.5 as compared to those values in the $(O/H)_{T_e}$ abundance distribution. The dispersion in $(O/H)_P$ abundance at fixed radius is rather small, ~ 0.08 dex, and is equal to that in $(O/H)_{T_e}$ abundance. The dispersion in $(O/H)_{R_{23}}$ abundance at fixed radius is appreciably larger, ~ 0.16 dex, compared to that in $(O/H)_{T_e}$ abundance. It has been shown that the extra dispersion in $(O/H)_{R_{23}}$ abundances is an artifact and reflects scatter in excitation parameter P at fixed radius.

Key words: Galaxies: abundances – Galaxies: ISM – Galaxies: spiral – Galaxies: individual: M101

A&A manuscript no.
(will be inserted by hand later)

Your thesaurus codes are:
missing; you have not inserted them

ASTRONOMY AND ASTROPHYSICS

The oxygen abundance distribution in M101

L.S. Pilyugin

Main Astronomical Observatory of National Academy of Sciences of Ukraine, Goloseevo, 03680 Kiev-127, Ukraine, (pilyugin@mao.kiev.ua)

Received 15 March 2001 / accepted 00 Month 2001

1. Introduction

By now spectra have been obtained for hundreds of H II regions in spiral galaxies. Accurate oxygen abundances can be derived from measurement of temperature-sensitive line ratios, such as [OIII]4959,5007/[OIII]4363. This method will be referred to as the T$_e$ - method. Unfortunately, in oxygen-rich H II regions the temperature-sensitive lines such as [OIII]4363 are too weak to be detected. For such H II regions, empirical abundance indicators based on more readily observable lines were suggested (Pagel et al. 1979; Alloin et al. 1979). The empirical oxygen abundance indicator R$_{23}$ = ([OII]3727,3729 + [OIII]4959,5007)/H$_\beta$, suggested by Pagel et al. (1979), has found widespread acceptance and use for the oxygen abundance determination in H II regions where the temperature-sensitive lines are undetectable. This method will be referred to as the R$_{23}$ - method. Using the R$_{23}$ - method, the characteristic oxygen abundances (the oxygen abundance at a predetermined galactocentric distance) and radial oxygen abundance gradients were obtained for a large sample of spiral galaxies (Vila-Costas and Edmunds (1992), Zaritsky et al. (1994), van Zee et al. (1998), among others).

However, the basic problem whether R$_{23}$ is an accurate abundance indicator is open for discussion (Zaritsky 1992, Kinkel and Rosa 1994, among others). It has been found (Pilyugin 2000 (Paper I)) that the error in the oxygen abundance derived with the R$_{23}$ – method involves two parts: the first is a random error and the second is a systematic error depending on the excitation parameter. A new way of oxygen abundance determination in H II regions (P – method) was suggested (Paper I, Pilyugin 2001 (Paper II)). By comparing oxygen abundances in high-metallicity H II regions derived with the T_e – method and those derived with the P – method, it was found that the precision of oxygen abundance determination with the P – method is comparable to that of the T_e – method (Paper II). It was shown that the R$_{23}$ – method provides more or less realistic oxygen abundances in high-excitation H II regions, but yields overestimates in low-excitation ones.

Taking into account this fact together with the fact known for a long time (Searle 1971, Smith 1975) that galaxies can show strong radial excitation gradients, in the sense that only low-excitation H II regions populate the central parts of some galaxies, one can expect that the central oxygen abundances and gradient slopes based on the (O/H)$_{R_{23}}$ data can be appreciably overestimated.

This speculation can have far-reaching implications (the empirical estimation of the oxygen yield, correlations of the behaviour of oxygen abundances with other properties of spiral galaxies, etc). This speculation can be verified by comparison of the radial (O/H)$_{R_{23}}$ abundance distribution with the radial (O/H)$_{T_e}$ abundance distribution. The well-observed spiral galaxy M101 provides such possibility.

The comparison between radial distributions of (O/H)$_{T_e}$, (O/H)$_P$, and (O/H)$_{R_{23}}$ abundances across the disk of M101 aiming to test the credibility of the (O/H)$_P$ and (O/H)$_{R_{23}}$ abundances is a goal of the present study.

2. The oxygen abundance distribution in M101

2.1. General comments

Despite the fact that the spectroscopic data with detections of diagnostic emission lines in H II regions makes it possible to determine the accurate oxygen abundance (O/H)$_{T_e}$, the oxygen abundances in the same H II region with measured line ratios [OIII]$\lambda\lambda 4959, 5007/\lambda 4363$ derived in different works can differ for three reasons: atomic data adopted, interpretation of the temperature structure (single characteristic T_e, two-zone model for T_e, model with small-scale temperature fluctuations) and errors in the line intensity measurements. Therefore the compilation of H II regions with original oxygen abundance determinations through the T$_e$ – method from different works carried out over more than twenty years is not a set of homogeneous determinations. Accordingly, the available published spectra of H II regions with measured line ratios [OIII]$\lambda\lambda 4959, 5007/\lambda 4363$ have been reanalysed to produce a homogeneous set. Two-zone models of H II regions with the algorithm for oxygen abundance determination

Send offprint requests to: L.S. Pilyugin

from Pagel et al. (1992) and T_e([OII]) – T_e([OIII]) relation from Garnett (1992) were adopted here.

The determination of the $(O/H)_P$ oxygen abundances in high-metallicity H II regions has been considered in Paper II. The following expression has been suggested

$$12+log(O/H)_P = \frac{R_{23} + 54.2 + 59.45P + 7.31P^2}{6.07 + 6.71P + 0.37P^2 + 0.243R_{23}}, (1)$$

where R_{23} =R_2 + R_3, $R_2 = I_{[OII]\lambda3727+\lambda3729}/I_{H\beta}$, $R_3 = I_{[OIII]\lambda4959+\lambda5007}/I_{H\beta}$, and P = R_3/R_{23}. Eq.(1) has been used here for the determination of the $(O/H)_P$ oxygen abundances.

Several workers have suggested calibrations of the R_{23} in terms of the oxygen abundance (Edmunds and Pagel 1984, McCall et al. 1985; Dopita and Evans 1986, Zaritsky et al. 1994, among others). The most frequently used calibration after Edmunds and Pagel (1984) has been adopted here for the determination of the $(O/H)_{R_{23}}$ oxygen abundances.

2.2. Radial oxygen abundance gradient

The nearby Sc galaxy M101 = NGC5457 has long served as the prototype system for studying the radial oxygen abundance gradients in disks. Spectroscopic observations of H II regions in M101 have been carried out by many investigators (Smith 1975; Shields and Searle 1978; Rayo, Peimbert, and Torres-Peimbert 1982; McCall, Rybski, and Shields 1985; Torres-Peimbert, Peimbert, and Fierro 1989; Garnett and Kennicutt 1994; Kinkel and Rosa 1994; Kennicutt and Garnett 1996; van Zee et al. 1998; Garnett et al. 1999).

The H II regions of M101 with measured temperature-sensitive line ratios are listed in Table 1. The name of H II region is reported in column 1. The oxygen abundance $(O/H)_{T_e}$ recomputed here is reported in column 2. Source of line intensities measurements is given in column 3. The fractional radius ρ, normalized to the disk isophotal radius ρ_0, is listed in column 4. The galactocentric distances were taken from Kennicutt and Garnett (1996). The electron temperatures T_e([OIII]) in H II regions (with one exception, H II region Searle 5) have been determined from the measurements of [OIII]$\lambda\lambda4959, 5007/\lambda4363$ line ratios, and the electron temperatures T_e([OII]) in H II regions have been derived from the T_e([OII]) – T_e([OIII]) relation of Garnett (1992). In the case of H II region Searle 5 the electron temperature T_e([OIII]) cannot be directly determined from observational data since the measurement of [OIII]$\lambda\lambda4959, 5007/\lambda4363$ line ratio is not available. Instead the temperature-sensitive lines [OII]$\lambda\lambda7320, 7330$ and [NII]$\lambda5755$ were detected in deep spectrophotometry of H II region Searle 5 (Kinkel and Rosa 1994). Then the electron temperature T_e([OIII]) in H II region Searle 5 has been derived from the T_e([OII]) – T_e([OIII]) relation of Garnett (1992) using the value of T_e([OII]) reported by Kinkel and Rosa (1994). The oxygen abundance in H II region Searle 5 based on the T_e([OII) is labeled with letter *a* in Table 1. The other value of oxygen abundance in H II region Searle 5 has been computed using the value of T_e([NII) from Kinkel and Rosa (1994) and assuming T_e([OII]) = T_e([NII]). The oxygen abundance in H II region Searle 5 based on the T_e([NII) is labeled with letter *b* in Table 1.

Table 1. Oxygen abundances in H II regions of spiral galaxy M101. The name of H II region is reported in column 1. The oxygen abundance computed here in common way (through the T_e – method) is reported in column 2. The oxygen abundances in H II region Searle 5 derived with T_e([OII) and T_e([NII) are labeled with letters a and b respectively. Source of line intensities measurements is given in column 3. The fractional radius ρ, normalized to the disk isophotal radius, is listed in column 4.

H II region	12+log(O/H)$_{T_e}$	reference	ρ
Searle 5	8.55[a]	KR94	0.22
	8.77[b]	KR94	
+252-107	8.55	M85	0.33
NGC5461	8.40	S75	0.34
	8.50	R82	
	8.42	T89	
NGC5455	8.40	S75	0.48
	8.52	SS78	
	8.43	T89	
-347+276	8.45	vZ98	0.54
-459-053	8.32	vZ98	0.55
NGC5447	8.34	S75	0.55
Searle 12	8.19	S75	0.67
-398-436	8.06	vZ98	0.68
NGC5471	7.99	S75	0.84
	8.17	SS78	
	8.18	R82	
	8.11	T89	
	8.10	G99	
H681	7.91	GK94	1.04
+010+885	7.96	vZ98	1.04

List of references:
G99 – Garnett, Shields, Peimbert, Torres-Peimbert, Skillman, Dufour, Terlevich E, Terlevich R, 1999 GK94 – Garnett, Kennicutt, 1994; KR94 – Kinkel, Rosa, 1994; M85 – McCall, Rybski, Shields, 1985; R82 – Rayo, Peimbert, Torres-Peimbert, 1982; S75 – Smith, 1975; SS78 – Shields, Searle, 1978; T89 – Torres-Peimbert, Peimbert, Fierro, 1989; vZ98 – van Zee, Salzer, Haynes, O'Donoghue, Balonek, 1998

In Fig.1a we show oxygen abundances $(O/H)_{T_e}$ (the filled circles) for H II regions from Table 1 as a function of galactocentric distance. As seen in Fig.1a the $(O/H)_{T_e}$ data is sufficient in quantity and quality for an accurate determination of the value of the oxygen abundance gradient within the M101. It is evident from Fig.1a that the radial distribution of oxygen abundance within the disk of

M101 can be reproduced by a single line. The best fit to the $(O/H)_{T_e}$ data is

$$12 + log(O/H)_{T_e} = 8.81(\pm0.08) - 0.028(\pm0.005)\ R_G, \quad (2)$$

where R_G is in kpc. The $(O/H)_{T_e}$ – R_G relation is presented by the solid line in Fig.1. The uncertainty of the value of central oxygen abundance is spesified by the mean deviation of positions of H II regions from the O/H – R_G relation. The maximum value of the error in the slope expressed in units of dex/ρ_0 (where ρ_0 is the isophotal radius) can be adopted equal to twice value of the mean deviation. The error in the slope expressed in units of dex/kpc can be estimated through the division of the error in the slope expressed in units of dex/ρ_0 by isophotal radius in kpc, that gives –0.028±0.005 dex/kpc.

Fig.1b shows the radial $(O/H)_P$ abundance distribution (the open circles) for H II regions from Kennicutt and Garnett (1996). The oxygen abundances in H II regions with galactocentric distances larger than ∼ 22 kpc are expected (Eq.2) to be less than 12+logO/H=8.2, i.e they do not belong to the upper branch of the R_{23} – O/H diagram. Since the Eq.(1) can be used for oxygen abundance determination in H II regions of the upper branch of the R_{23} – O/H diagram only, the H II regions of M101 with galactocentric distances larger than 22 kpc are not presented in Fig.1b. The best fit to the $(O/H)_P$ data is

$$12 + log(O/H)_P = 8.76(\pm0.08) - 0.024(\pm0.005)\ R_G. \quad (3)$$

This $(O/H)_P$ – R_G relation is shown by the dashed line in the Fig.1b. The mean residual from the $(O/H)_P$ – R_G relation is 0.084 dex. The corresponding error in the slope is ±0.005 dex/kpc, i.e. the same as in the case of gradient traced by the $(O/H)_{T_e}$ abundances. Inspection of Fig.1b shows that the radial $(O/H)_P$ abundance distribution is in agreement with the $(O/H)_{T_e}$ distribution.

Fig.1c shows the radial $(O/H)_{R_{23}}$ abundance distribution (the open squares) for the same H II regions as in Fig.1b. The best fit to the $(O/H)_{R_{23}}$ data is

$$12 + log(O/H)_{R_{23}} = 9.23(\pm0.16) - 0.044(\pm0.010)\ R_G. \quad (4)$$

This $(O/H)_{R_{23}}$ – R_G relation is shown by the dotted line in Fig.1c. The mean residual from the $(O/H)_{R_{23}}$ – R_G relation is 0.16 dex. The corresponding error in the slope is ±0.010 dex/kpc. Inspection of Fig.1c shows that the $(O/H)_{R_{23}}$ abundances in H II regions with large galactocentric distances are close to the $(O/H)_{T_e}$ – R_G relation, while the $(O/H)_{R_{23}}$ abundances in H II regions in the inner part of M101 have significant deviations from the $(O/H)_{T_e}$ – R_G relation. This behaviour of $(O/H)_{R_{23}}$ abundances with galactocentric distance confirms the conclusion of Paper II that the R_{23} calibration of Edmunds and Pagel (1984) provides a realistic oxygen abundances in high-excitation H II regions, but overestimates them in low-excitation ones. Indeed, the H II regions with galactocentric distances larger than around 17 kpc are high- and moderate-excitation (P values are higher than around 0.6) ones, Fig.1d, their $(O/H)_{R_{23}}$ abundances are close to the $(O/H)_{T_e}$ – R_G relation. By contrast, the H II regions with galactocentric distances smaller than around 9 kpc are

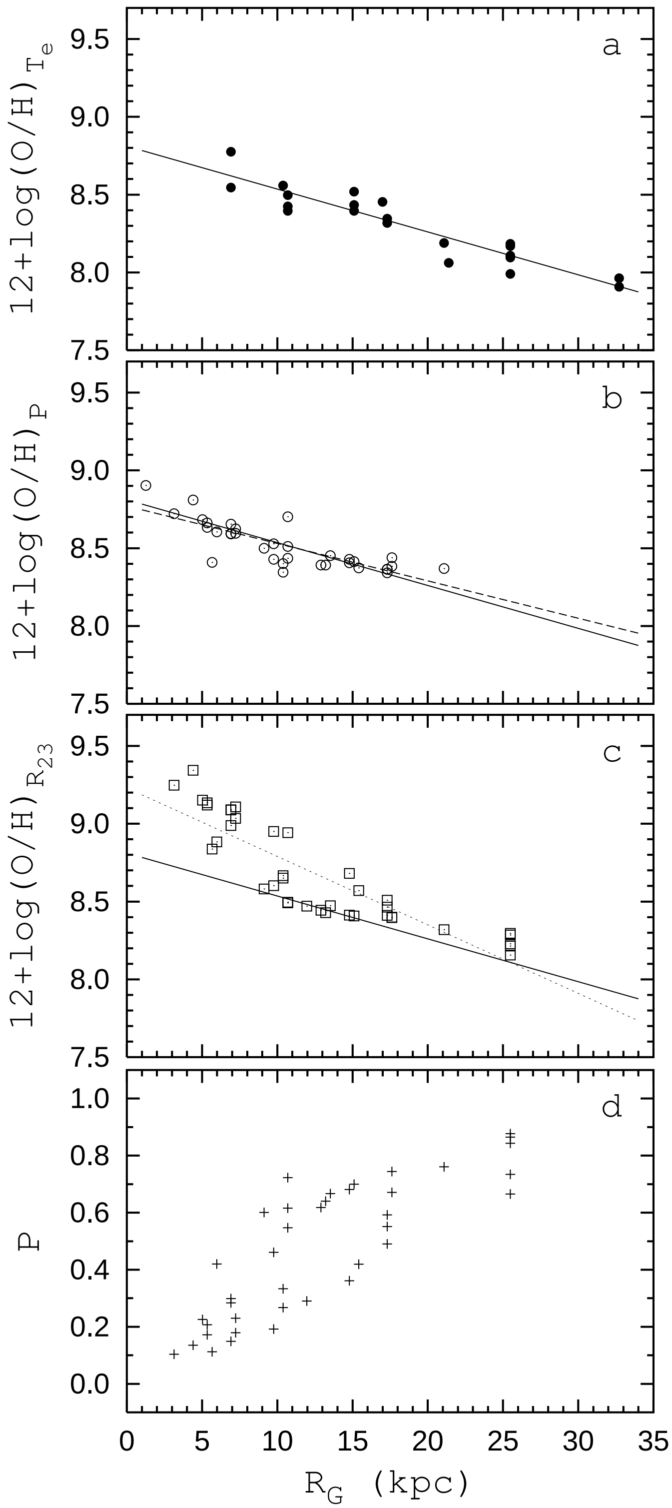

Fig. 1. Gradients in the properties of M101. **a)** The $(O/H)_{T_e}$ abundance distribution (filled circles) and the best fit (solid line). **b)** The $(O/H)_P$ abundance distribution (open circles) and the best fit (dashed line). The solid line is the $(O/H)_{T_e}$ – R_G relation. **c)** The $(O/H)_{R_{23}}$ abundance distribution (open squares) and the best fit (dotted line). The solid line is the $(O/H)_{T_e}$ – R_G relation. **d)** The excitation parameter P as a function of galactocentric distance.

low-excitation (P values are less than around 0.3) ones, Fig.1d, their $(O/H)_{R_{23}}$ abundances have significant deviations from the $(O/H)_{T_e}$ – R_G relation.

The form of oxygen abundance gradient in M101 has been investigated in a number of studies (Evans 1986, Vila-Costas and Edmunds 1992, Henry and Howard 1995, Kennicutt and Garnett 1996). It has been noted by Kennicutt and Garnett (1996) and Roy and Walsh (1997) that the shape of the $(O/H)_{R_{23}}$ distribution is very sensitive to the precise form of the R_{23} calibration. In the case of M101 Kennicutt and Garnett (1996) have found that the Edmunds and Pagel (1984) calibration produces a "steep – shallow" break in the slope of the distribution (see also Vila-Costas and Edmunds 1992), while the Dopita and Evans (1986) and McCall et al. (1985) calibrations yield distributions which are very well fitted with a single exponential function, though the slope of the exponential differs considerably between the two calibrations. A careful examination of Fig.1 suggests that the distributions of the $(O/H)_{T_e}$, Fig.1a, and $(O/H)_P$ abundances, Fig.1b, can be fitted quite comfortably within the scatter by the same exponential with constant slope. There is hint of a turnover in the slope of the $(O/H)_{R_{23}}$ abundance distribution, Fig.1c. This turnover is artifact and reflects the increase of error in $(O/H)_{R_{23}}$ abundance with decrease of galactocentric distance caused by variations in excitation parameter, Fig.1d.

An important result of the present study is the rather low value of the central oxygen abundance in M101. This is in agreement with the result of Kinkel & Rosa (1994), who showed the need to lowering all H II region abundances obtained on the basis of the R_{23} calibration after Edmunds and Pagel (1984) by at least 0.2 at intrinsic solar like O/H values and above. One more large spiral galaxy in which the $(O/H)_{T_e}$ abundance distribution has been established is the Milky Way Galaxy. Caplan et al (2000) and Deharveng et al (2000) have analysed Galactic H II regions and have obtained the slope −0.0395 dex/kpc with central oxygen abundance 12+log(O/H) = 8.82, close to the solar value $12+\log(O/H)_{\odot} = 8.83$ (Grevesse and Sauval 1998), and 12+log(O/H) = 8.48 at the solar galactocentric distance, around a factor of 2 lower than the solar abundance. Rodriques (1999) has considered seven bright Galactic H II regions with galactocentric distances in the range 6 – 10 kpc and has found that all the H II regions studied are characterized by similar abundances, $12+\log(O/H) \sim 8.45\pm0.1$. This value of the oxygen abundance at the solar radius is close to the value of the interstellar oxygen in the vicinity of the Sun which is about two-thirds of the solar oxygen abundance (Meyer et al. 1998). Those data taken together suggest that the oxygen abundance at the solar radius is $1/2 \div 2/3$ of the solar oxygen abundance and increases up to about solar value in the centre of our Galaxy. The central oxygen abundance in M101 based on the $(O/H)_{T_e}$ (or $(O/H)_P$) abundances is close to that in our Galaxy.

Thus, the consideration of M101 suggests the following. The available $(O/H)_{T_e}$ abundances allow to establish quite firmly the parameters of the radial oxygen abundance distribution (the central oxygen abundance and the gradient) within M101. The parameters of the $(O/H)_P$ abundance distribution are close to those of the $(O/H)_{T_e}$ abundance distribution. The parameters of the $(O/H)_{R_{23}}$ abundance distribution differ significantly from those of the $(O/H)_{T_e}$ abundance distribution: the values of the gradient and the central oxygen abundance based on the $(O/H)_{R_{23}}$ data are overestimated as compared to values derived from the $(O/H)_{T_e}$ distribution.

2.3. The dispersion in abundance

The dispersion in $(O/H)_P$ abundance at fixed radius is coincident with that in $(O/H)_{T_e}$ abundance, ~ 0.08 dex. In the general case, the error in line intensity measurements can make contribution to the scatter at fixed galactocentric distance. The precision of present-day determinations of the oxygen abundances in high-metallicity H II regions through the T_e – method seems to be about 0.1dex (Deharveng et al. 2000). The precision of oxygen abundance determination with the P – method is comparable to that of the T_e – method (Paper II). Those facts taken together suggest none, or only marginal, scatter at a given galatocentric distance. However, Kennicutt and Garnett (1996) advocate that the quality of their specta is sufficiently high that observational errors contribute negligibly to the dispersion. If this is the case it cannot be excluded that some part of the dispersion in $(O/H)_P$ abundance reflects the actual deviations of oxygen abundances in individual H II regions from the general $(O/H)_P$ – R_G trend.

The dispersion in $(O/H)_{R_{23}}$ abundance at fixed radius, ~ 0.16 dex, is appreciable larger than that in $(O/H)_P$ abundance, ~ 0.08 dex. The following interpretation of this fact can be suggested. The extra dispersion in $(O/H)_{R_{23}}$ abundance at fixed radius is an artifact and reflects the dispersion in excitation parameter P.

Kennicutt and Garnett (1996) have also suggested that the dispersion in $(O/H)_{R_{23}}$ abundance at fixed radius can be attributed partly to variations in excitation parameter, but they did not find a firm confirmation of this suggestion. Following the strategy of Kennicutt and Garnett we fitted the radial variations in $\log(O/H)_{R_{23}}$ and P by linear relations and considered correlation between the residuals in $\log(O/H)_{R23}$ and P. This correlation is shown in Fig.2 by pluses. As can seen in Fig.2 the correlation between the residuals is very weak, if at all. Why? We will demonstrate that this is due to two reasons; *i)* abundance dispersion in the H II regions themselves, and *ii)* a feature of the sample.

Fig.3 shows $\delta(O/H)_{R_{23}}$ (the deviation of individual $\log(O/H)_{R_{23}}$ from $\log(O/H)_P$ – R_G fit, Eq.3) versus $\Delta(O/H)_P$ (the $\log(O/H)_P$ residual from the same fit) for H II regions from Kennicutt and Garnett (1996). The triangles are H II regions with P>0.5, the pluses are H II re-

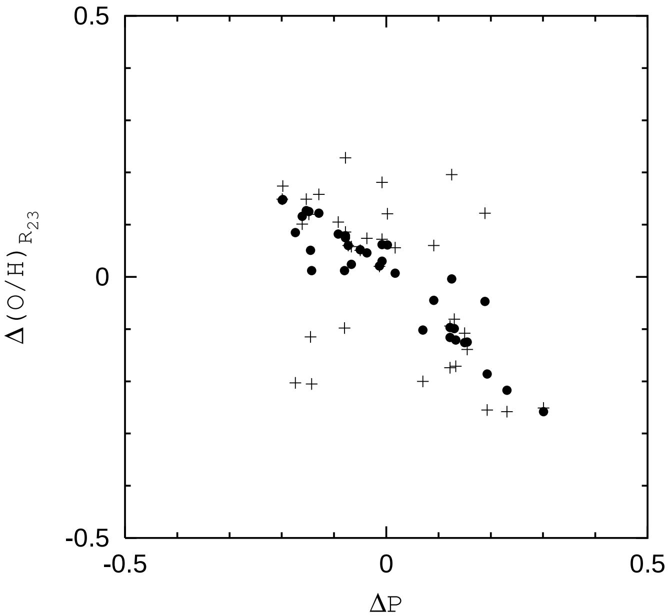

Fig. 2. The $\log(O/H)_{R_{23}}$ residual from a mean linear fit, $\Delta(O/H)_{R_{23}}$, as a function of excitation parameter P residual, ΔP, for H II regions from Kennicutt and Garnett (1996). The data obtained with original $(O/H)_{R_{23}}$ are shown by pluses, the data obtained with corrected $(O/H)_{R_{23}}$ are shown by filled circles.

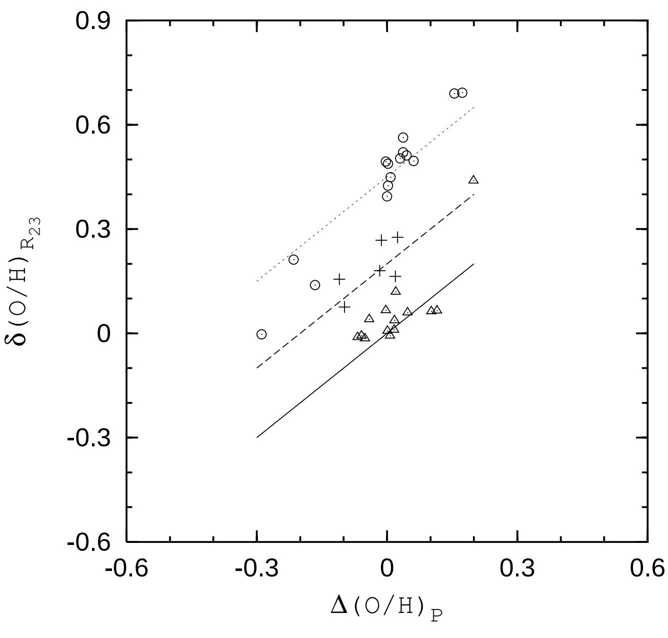

Fig. 3. The $\delta(O/H)_{R_{23}}$ is the deviation of $\log(O/H)_{R_{23}}$ from the $\log(O/H)_P$ – R_G fit. The $\Delta(O/H)_P$ is the $\log(O/H)_P$ residual from the same fit. The triangles are H II regions with P>0.5, the pluses are H II regions 0.5>P>0.3, the circles are those with 0.3>P. The solid line is the relation $\delta(O/H)_{R_{23}} = \Delta(O/H)_P$, the dashed line is the relation $\delta(O/H)_{R_{23}} = \Delta(O/H)_P + 0.2$, the dotted line is the relation $\delta(O/H)_{R_{23}} = \Delta(O/H)_P + 0.45$.

gions 0.5>P>0.3, the circles are those with 0.3>P. Fig.3 shows that the variations in excitation parameter P (from $\sim$ 0.9 to $\sim$ 0.1, see Fig.1d) result in the difference in $(O/H)_{R_{23}}$ as large as $\sim$ 0.6dex. Fig.3 shows that in the general case the $\delta(O/H)_{R_{23}}$ is the sum of two parts; the first is the $\Delta(O/H)_P$ and the second is the deviation depending on the value of excitation parameter P.

The relevant feature of the sample of H II regions of M101 from Kennicutt and Garnett (1996) can be seen in Fig.1d; the H II regions occupy a relatively narrow band in the P – R_G diagram. Due to this feature of the sample of H II regions the variations in excitation parameter P at fixed galactocentric distance do not exceed $\sim$ 0.4, or the maximum deviation of excitation parameter from mean value is around ±0.2. The maximum deviation around ±0.15dex in $(O/H)_{R_{23}}$ corresponds to this maximum deviation of excitation parameter. Thus, the expected *maximum* deviation in $(O/H)_{R_{23}}$ due to the deviation of excitation parameter from mean value is only twice the *average* actual deviation of oxygen abundances in individual H II regions from general $(O/H)_P$ – R_G trend, that can mask the correlation between the residuals in $\log(O/H)_{R23}$ and P. Therefore the $(O/H)_{R_{23}}$ values were corrected for deviations caused by dispersion in the H II regions themselves

$$(O/H)^c_{R_{23}} = (O/H)_{R_{23}} - \Delta(O/H)_P. \quad (5)$$

The ΔP – $\Delta(O/H)^c_{R_{23}}$ diagram for corrected $(O/H)^c_{R_{23}}$ values has been constructed. This diagram is shown in Fig.2 by filled circles. As can seen in Fig.2 the correlation between the residuals is rather tight in this case. This is reliable confirmation that the dispersion in $(O/H)_{R_{23}}$ abundance at fixed radius is caused partly by variations in excitation parameter.

As for the feature of Kennicutt and Garnett's sample of H II regions, the lack of high-excitation H II regions in central part of M101 can be explained by the ionization temperature gradient. The radial distribution of the ionization temperature for the H II regions in M101 has been investigated by Vilchez and Pagel (1988). They showed that there is a clear gradient in the temperature along the disk of M101. The data for other galaxies confirm the softening of the ionizing spectra with increasing metal abundance (Kennicutt et al. 2000, and references therein). Fig.4 shows the P – $(O/H)_P$ diagram for a large sample of H II regions from Zaritsky et al. (1994) and van Zee et al. (1998). Examination of Fig.4 shows that the maximum value of the excitation parameter P is dependent on the metallicity. Since excitation parameter P is an indicator of hardness of the ionizing radiation, the P – $(O/H)_P$ diagram for large sample of H II regions confirms the softening of the ionizing spectra with increasing metal abundance. But the lack of low-excitation H II at outer part of M101 seems to be conditioned by selection.

Kennicutt and Garnett (1996) concluded that there is hint that some of the dispersion in $(O/H)_{R_{23}}$ abundances in M101 is the result of a large-scale deviation from azimuthal symmetry. Is there spatial asymmetry in $(O/H)_P$

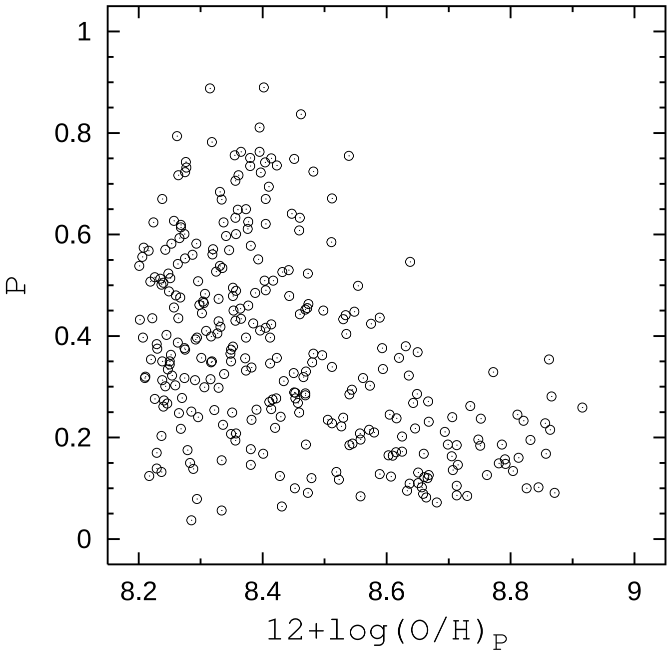

Fig. 4. The P – $(O/H)_P$ diagram for H II regions from Zaritsky et al. (1994) and van Zee et al. (1998).

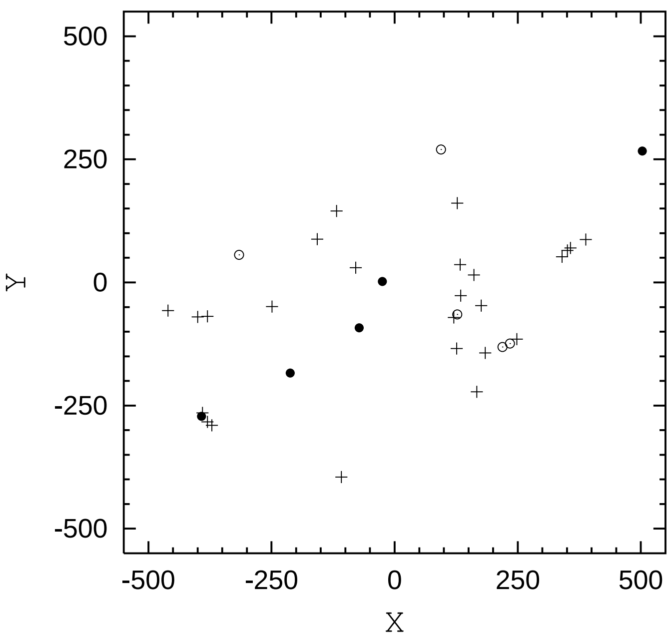

Fig. 5. The spatial distribution of the abundance residuals. Pluses are H II regions with -0.08 < $\Delta(O/H)_P$ < 0.08, filled circles are those with $\Delta(O/H)_P$ > 0.08, open circles are those with $\Delta(O/H)_P$ < -0.08.

abundance residuals? Fig.5 shows the spatial distribution of $(O/H)_P$ abundance residuals. Pluses are H II regions with -0.08 < $\Delta(O/H)_P$ < 0.08, filled circles are those with $\Delta(O/H)_P$ > 0.08, open circles are those with $\Delta(O/H)_P$ < -0.08. Indeed, some asymmetry in the spatial distribution of $(O/H)_P$ abundance residuals can be seen in Fig.5. However, following Kennicutt and Garnett (1996) we can conclude that more data are needed to test whether this asymmetry is real.

3. Conclusions

The radial distributions of the oxygen abundances determined in three different ways (with the classic T_e – method, with the R_{23} – method, and with the P – method) in H II regions of large spiral galaxy M101 have been compared.

It has been found that the available $(O/H)_{T_e}$ abundances are sufficient in quantity and quality for an accurate determination of the parameters of the radial abundance distribution (the central oxygen abundance and the gradient). We found that $12+\log(O/H)_{T_e} = 8.81(\pm0.08) - 0.028(\pm0.005)R_G$(kpc).

It has been found that the parameters of the radial $(O/H)_P$ abundance distribution are close to those of the $(O/H)_{T_e}$ abundance distribution. We obtained that $12+\log(O/H)_P = 8.76(\pm0.08) - 0.024(\pm0.005)R_G$(kpc). This confirms the conclusion of Paper II that the $(O/H)_P$ abundances are as credible as the $(O/H)_{T_e}$ abundances.

It has been obtained that the parameters of the radial $O/H_{R_{23}}$ abundance distribution differ significantly from those of the O/H_{T_e} abundance distribution. We found that $12+\log(O/H)_{R_{23}} = 9.23(\pm0.16) - 0.044(\pm0.010)R_G$(kpc). This confirms our speculation that the central oxygen abundance and gradient slope based on the $(O/H)_{R_{23}}$ data can be appreciably overestimated.

The dispersion in $(O/H)_{R_{23}}$ abundance at fixed radius is appreciable larger than that in $(O/H)_P$ abundance. It has been demonstrated that the extra dispersion in $(O/H)_{R_{23}}$ abundance is an artifact and reflects the dispersion in excitation parameter P.

Acknowledgements. It is a pleasure to thank J.M. Vilchez and D.R. Garnett for their helpful comments on this work. I thank the referee, Prof. B.E.J. Pagel, for helpful c omments and suggestions as well as improving the English text. This study was partly supported by the NATO grant PST.CLG.976036 and the Joint Research Project between Eastern Europe and Switzerland (SCOPE) No. 7UKPJ62178.

References

Alloin D., Collin-Souffrin S., Joly M., Vigrough L., 1979, A&A 78, 200

Caplan J., Deharveng L., Pena M., Costero R., Blondel C., 2000, MNRAS 311, 317

Deharveng L., Pena M., Caplan J., Costero R., 2000, MNRAS 311, 329

Dopita M.A., Evans I.N., 1986, ApJ 307, 431

Edmunds M.G., Pagel B.E.J., 1984, MNRAS 211, 507

Evans I.N., 1986, ApJ 309, 544

Garnett D.R., 1992, AJ 103, 1330

Garnett D.R., Kennicutt R.C., 1994, ApJ 426, 123

Garnett D.R., Shields G.A., Peimbert M., Torres-Peimbert S., Skillman E.D., Dufour R.J., Terlevich E., Terlevich R.J., 1999, ApJ 513, 168
Grevesse N., Sauval A.J., 1998, in: Solar composition and its evolution – from core to corona, Eds. Fronlich G., Huber M.C.E., Solanki S.K., von Steiger R. (Kluwer, Space Sciences Series of ISSI, vol. 5), p. 161
Henry R.B.C., Howard J.W., 1995, ApJ 438, 170
Kennicutt R.C., Bresolin F., French H., Martin P., 2000, ApJ 537, 589
Kennicutt R.C., Garnett D.R., 1996, ApJ 456, 504
Kinkel U., Rosa M.R., 1994, A&A 282, L37
McCall M.L., Rybski P.M., Shields G.A., 1985, ApJSS 57, 1
Meyer D.M., Jura M., Cardelli J.A., 1998, ApJ 493, 222
Pagel B.E.J., Edmunds M.G., Blackwell D.E., Chun M.S., Smith G., 1979, MNRAS 189, 95
Pagel B.E.J., Simonson E.A., Terlevich R.J., Edmunds M.G., 1992, MNRAS 255, 325
Pilyugin L.S., 2000, A&A 362, 325 (Paper I)
Pilyugin L.S., 2001, A&A 369, 594 (Paper II)
Rayo J.F., Peimbert M., Torres-Peimbert S., 1982, ApJ 255, 1
Rodriguez M., 1999, A&A 351, 1075
Roy J.-R., Walsh J.R., 1997, MNRAS 288, 715
Searle L., 1971, ApJ 168, 327
Shields G.A., Searle L., 1978, ApJ 222, 821
Smith H.E., 1975, ApJ 199, 591
Torres-Peimbert S., Peimbert M., Fierro J., 1989, ApJ 345, 186
van Zee L., Salzer J.J., Haynes M.P., O'Donoghue A.A., Balonek T.J., 1998, AJ 116, 2805
Vila-Costas M.B., Edmunds M.G., 1992, MNRAS 259, 121
Vilchez J.M., Pagel B.E.J., 1988, MNRAS 231, 257
Zaritsky D., 1992, ApJLet 390, L73
Zaritsky D., Kennicutt R.C., Huchra J.P., 1994, ApJ 420, 87